

Article

# Investigation of Fluids in Macrocrystalline and Microcrystalline Quartz in Agate Using Thermogravimetry-Mass-Spectrometry

Julia Richter-Feig <sup>1</sup>, Robert Möckel <sup>2</sup>, Jens Götze <sup>1</sup> and Gerhard Heide <sup>1,\*</sup>

<sup>1</sup> TU Bergakademie Freiberg, Institute of Mineralogy, Brennhausgasse 14, 09596 Freiberg, Germany; richterjulia1989@gmail.com (J.R.-F.); jens.goetze@mineral.tu-freiberg.de (J.G.)

<sup>2</sup> Helmholtz-Zentrum Dresden-Rossendorf, Helmholtz Institute Freiberg for Resource Technology, Chemnitz Str. 40, 09599 Freiberg, Germany; r.moeckel@hzdr.de

\* Correspondence: richterjulia1989@gmail.com

Received: 3 November 2017; Accepted: 14 February 2018; Published: 17 February 2018

**Abstract:** Gaseous and liquid fluids in agates (banded chalcedony—SiO<sub>2</sub>) of different localities were investigated systematically by thermogravimetry-mass-spectrometry within a temperature range from 25 to 1450 °C, for the first time. Chalcedony and macrocrystalline quartz from twelve agate samples were investigated, from Germany (Schlottwitz, St. Egidien, Chemnitz and Zwickau), Brazil (Rio Grande do Sul), Scotland (Ayrshire) and the USA (Montana). They originate from mafic and felsic volcanic rocks as well as hydrothermal and sedimentary environments. The results were evaluated regarding compounds of hydrogen with fluorine, chlorine, nitrogen, carbon and sulphur. Additionally, oxygen compounds were recognized with hydrogen, fluorine, nitrogen, sulphur and carbon. The nature of the compounds was identified based on their mass-charge-ratio and the intensity ratios of the associated fragments. Due to interferences of different compounds with the same mass-charge-ratio, only H<sub>2</sub>O, HF, NO, S, SO, CO<sub>3</sub>—as well as several hydrocarbon compounds (for example CO<sub>3</sub><sup>2-</sup> or CO)—could be properly identified. The main degassing temperatures were detected at around 500 and 1000 °C. Generally, a difference between quartz and chalcedony regarding the composition of their fluids could not be found. The results indicate a silica source for the agate formation from aqueous solutions but also a possible role of fluorine compounds. Additionally, CO<sub>2</sub> and other fluids were involved in the alteration of volcanic rocks and the mobilization and transport of SiO<sub>2</sub>.

**Keywords:** agate; quartz; chalcedony; thermogravimetry-mass-spectrometry; EGA

## 1. Introduction

Agates (banded chalcedony—SiO<sub>2</sub>) are spectacular products of nature, which have been investigated for decades regarding the conditions of their formation (e.g., [1–10]). In detail, agates have a very complex composition consisting of certain SiO<sub>2</sub> polymorphs and morphological quartz varieties (e.g., [4,11–13]). For instance, quartzine, opal-A, opal-CT and/or moganite can be intergrown or intercalated with chalcedony layers and macrocrystalline quartz in agate. Moreover, agates can contain considerable amounts of water (molecular water and/or silanol groups) and mineral inclusions, which are often responsible for the different colouration of agates [4,7,12–14].

The process of agate formation is as complex as its composition and may differ depending on the type of parent rocks and formation environment. Most agates occur in volcanic host rocks.

The chemical and mineralogical composition of agates in volcanic host rocks as well as their association with certain mineral products of alteration processes (e.g., zeolites, clay minerals, iron oxides) led to the conclusion that the formation of these agates is closely connected to late-

and post-volcanic alteration or weathering of the parent rocks (e.g., [6–11]). The complex processes lead to the accumulation of silica in cavities, so that agates represent a mixture of certain SiO<sub>2</sub> polymorphs and morphological quartz varieties (e.g., [4,7,11,12]).

Transport and accumulation of silica in cavities of the host rocks is predominantly realized by diffusion processes. In basic volcanics, vesicular cavities form during the solidification of the lava, whereas in acidic volcanics so-called lithophysae (high-temperature crystallization domains [15]) are formed at first, due to the devitrification and degassing of the volcanic glass/melt.

The formation of vein agates is related to fissures and veins within different types of crystalline rocks, which enable a free movement of silica-bearing mineralizing fluids through a system of cracks. Here, SiO<sub>2</sub> is accumulated by hydrothermal-magmatic solutions, whereas silica in sedimentary agates preferentially derives from SiO<sub>2</sub>-rich pore solutions [16].

The accumulation and condensation of silicic acid result in the formation of silica sols and amorphous silica as precursors for the development of the typical agate structures. It is assumed that the formation of the typical agate microstructure is governed by processes of self-organization, starting with the spherulitic growth of chalcedony and continuing into chalcedony fibres [10,12]. Macrocrystalline quartz crystallizes when the SiO<sub>2</sub> concentration in the mineralizing fluid is low. The estimation of the temperature of agate formation using oxygen isotopes, Al concentrations or homogenization temperatures of fluid inclusions provided a temperature range between ca. 20 and 200 °C [7].

Although much geochemical and mineralogical data of agates exist, there are still open questions and controversial discussions, especially regarding the transport of the enormous amounts of silica necessary for the formation of agates. In general, it is assumed that diffusion of monomeric silicic acid in pore fluids could be the main transport process (e.g., [1,7,17,18]). However, geochemical data indicate that a transport of elements and chemical compounds in aqueous fluids cannot be the only process involved in agate formation. In certain agates (especially those of acidic volcanic rocks), elevated concentrations of Ge (>10 ppm), U (>15 ppm) and B (>30 ppm) as well as the occurrence of paragenetic calcite and fluorite indicate that other fluids can play a role in the alteration of volcanic rocks and the mobilization and transport of SiO<sub>2</sub> and other chemical compounds [11,19]. In consequence, additional chemical transport reactions (CTR) of gases and liquids by stable fluorine (and chlorine) compounds such as SiF<sub>4</sub>, BF<sub>3</sub>, GeF<sub>4</sub> and UO<sub>2</sub>F<sub>2</sub> could explain the processes during agate formation better than exclusive element transport by silicic acid in aqueous solutions (e.g., [20,21]). The analysis of the fluids in the different agates provides information about the chemical composition of mineral-forming fluids and for the reconstruction of the agate formation processes.

The sample material includes agates from basic and acidic volcanic rocks, hydrothermal vein agates and agates of sedimentary origin to enable a comparison of these different formation environments. In the present study, a systematic study of gaseous and liquid fluids in agates from different localities and of different origin was performed by evolved gas analysis (in this case and further called thermogravimetry-mass-spectrometry). Moreover, microcrystalline chalcedony and macro-crystalline quartz were analysed separately to reveal possible differences in the fluid composition. Because of the lack of visible fluid inclusions within the micro-crystalline agate matrix, conventional techniques for the characterization of the fluids such as microscopy or Raman spectroscopy could not be applied.

## 2. Materials and Methods

### 2.1. Sample Material

In the present study, agates from eight different localities and different geological environments were analysed (Table 1, Figure 1), five from Saxony/Germany (Chemnitz-Furth, Chemnitz-Altendorf, Schlottwitz, St. Egidien and Zwickau) and each one from Brazil, Scotland and the USA, respectively. The material includes samples from basic, intermediate and acidic volcanic host rocks as well as

hydrothermal vein agate and agate of sedimentary origin. Twenty-two measurements in total were made including multiple measurements on some samples.

**Table 1.** Compilation of the investigated agate samples and their genetic types.

Location	Genetic Type	Age of Host Rock	Measurements Per Sample	Reference
Soledade (Rio Grande do Sul, Brazil)	Basic volcanic rock (basalt)	~135 Ma	2	[22]
Heads of Ayr (Dunure area, Scotland)	Basic volcanic rock (basalt)	~412 Ma	2	[23,24]
Zwickau-Planitz (Saxony, Germany)	Acidic volcanic rock (pitchstone)	~290 Ma	2	[19]
St.Egidien (Saxony, Germany)	Acidic volcanic rock (ignimbrite)	~290 Ma	6	[19]
Chemnitz-Furth (Saxony, Germany)	Acidic volcanic rock (ignimbrite)	~290 Ma	4	[19]
Chemnitz-Altendorf (Saxony, Germany)	Vein agate in altered Pitchstone	~290 Ma	2	[19]
Schlottwitz (Saxony, Germany)	Hydrothermal vein agate	~270 Ma	2	[25]
Dryhead area, Prior Mountains (Montana, USA)	Sedimentary agate (clay shale and siltstone)	250–300 Ma	2	[26]

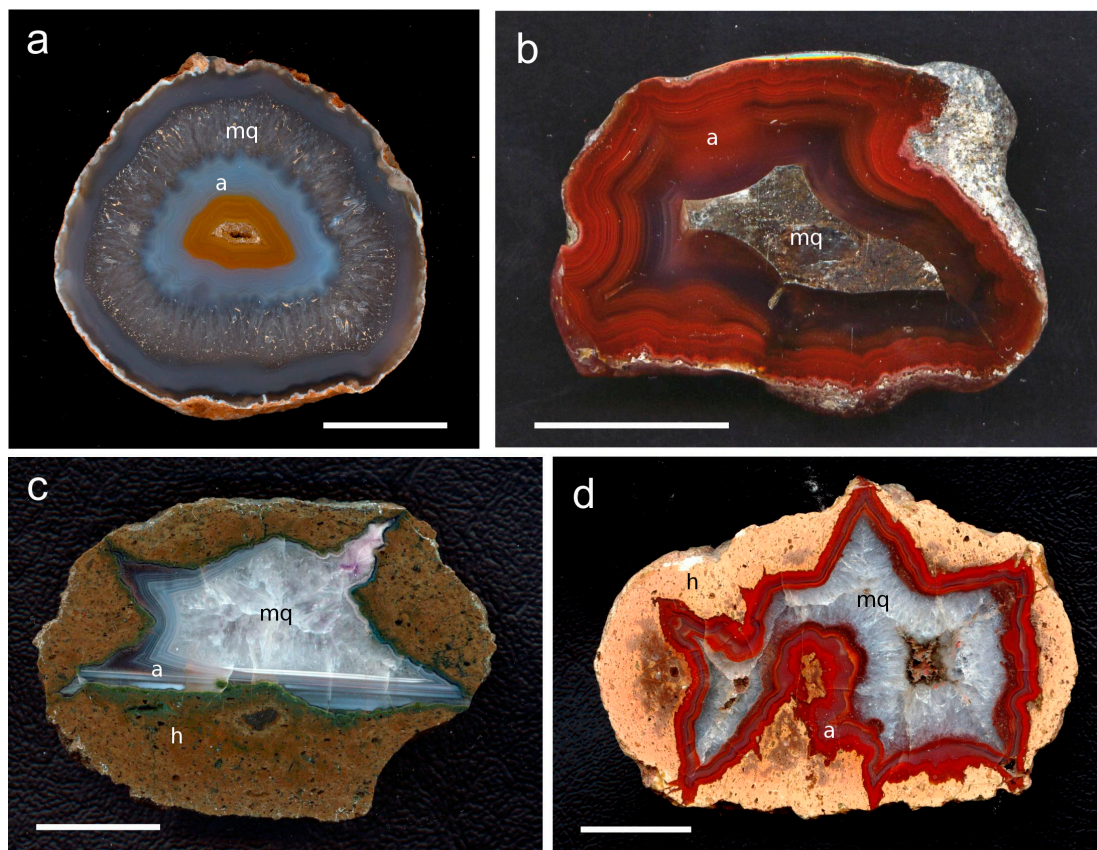


**Figure 1.** Cont.

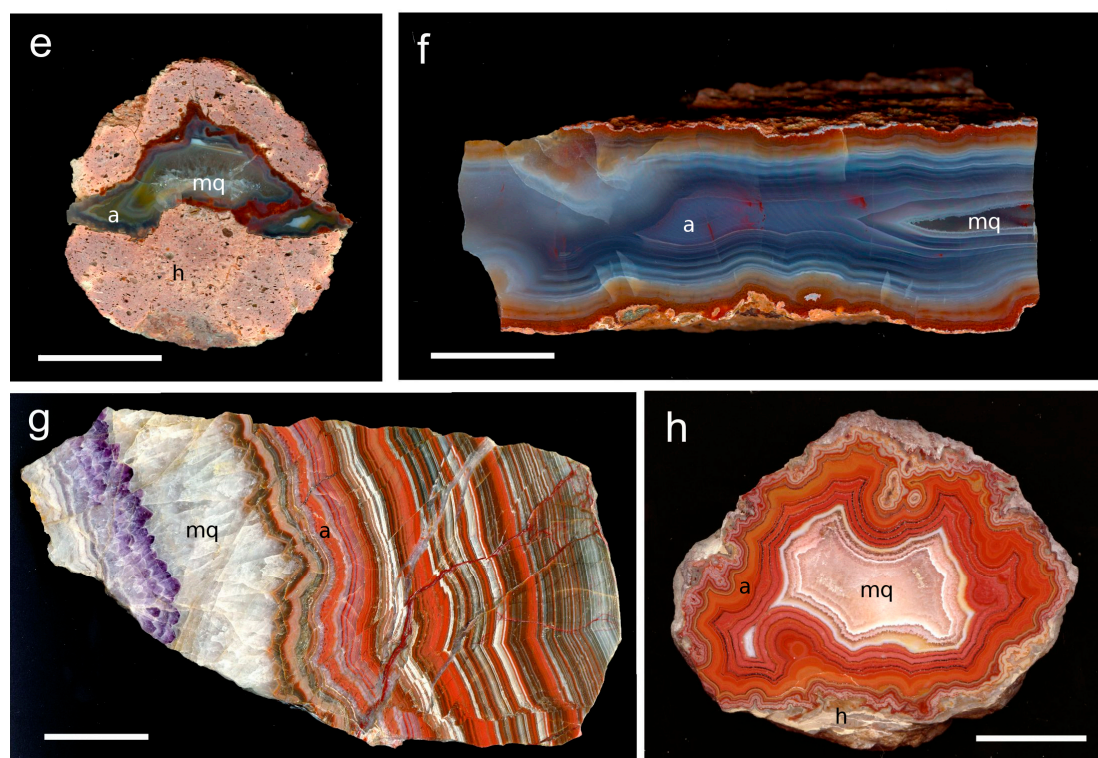


**Figure 1.** Investigated agate samples of the present study with a = agate, mq = macrocrystalline quartz, h = host rock; (a) Soledade, Rio Grande do Sul (Brazil), (b) Heads of Ayr, Dunure area (Scotland), (c) Zwickau-Planitz, Saxony (Germany), (d) St. Egidien, Saxony (Germany), (e) Chemnitz-Furth, Saxony (Germany), (f) Chemnitz-Altendorf, Saxony (Germany), (g) Schlottwitz, Saxony (Germany), (h) Dryhead area, Montana (USA); scale bar is 2 cm.

The sample material was crushed with a small steel hammer to a size between 0.4 and 1 mm and then handpicked under a binocular microscope in order to separate the quartz and chalcedony parts of the samples and to avoid impurities and mineral inclusions.

## 2.2. Analytical Method

The method of thermogravimetry-mass-spectrometry is based on temperature dependent changes of the physical properties of a substance [27]. Fluids and gases, which are included in a solid, can be released during heating. In order to analyse escaping fluids, the thermo-balance (with evacuated oven chamber) is directly coupled with a mass spectrometer [27].

This analytical arrangement enables a faster analysis and prevents reactions of the released gases as the distance between sample and mass-spectrometer is kept as short as possible [28].

The gases are ionized in an ionization chamber and then separated and measured according to their mass-charge ratio [29]. The equipment used in this study was a thermo-analytic system NETZSCH STA 409 (Netsch, Selb, Germany), directly coupled to a QMS 403/5 quadrupole mass spectrometer (Pfeiffer Vacuum, Aßlar, Germany) (Figure 2). A background measurement under similar conditions was taken prior to a set of three to five sample measurements.

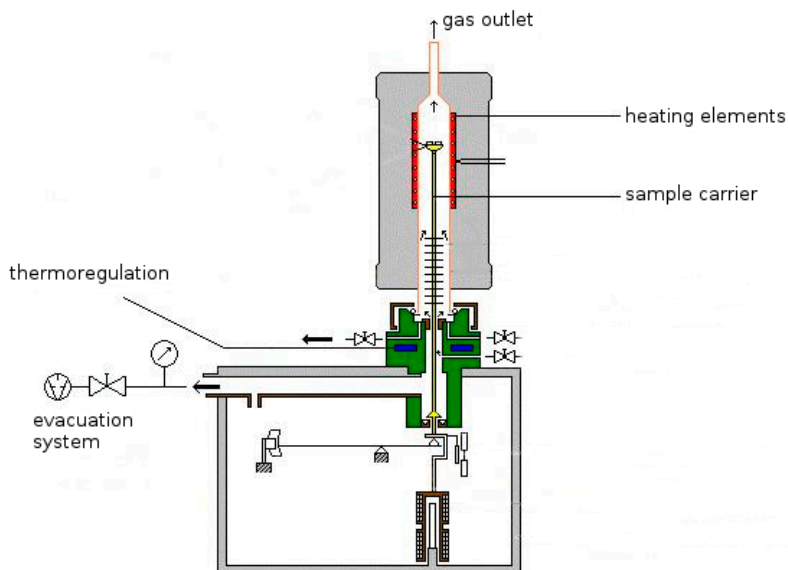


**Figure 2.** Schematic diagram of the apparatus NETZSCH STA 409. The gas outlet is directly coupled to the quadrupole mass-spectrometer.

Thirty milligram sample material were heated under vacuum ( $<10^{-5}$  mbar) up to a temperature of 1450 °C with a constant heating-rate of 10 K/min. For correct temperature measurements, the thermo-element is located directly beneath the sample holder.

### 3. Results

The focus of this investigation was the characterization of the compounds that escaped during heating at various temperatures. They were identified according to their mass-charge-ratio and the corresponding intensity relations of the associated fragments. The detected and measured fluids consisted of compounds of fluorine, chlorine, sulphur, carbon and nitrogen with oxygen and/or hydrogen.

By default, the thermographic curves were also logged, revealing total mass losses during heating to 1450 °C between 0.5% and 1.5% for chalcedony and  $<0.5\%$  for the quartz samples. Some similarities are found between the samples: chalcedony tends to have a rather unspecific mass loss during heating, with two main loss ranges between 100–500 °C and above 1000 °C (e.g., Chemnitz-Furth, Chemnitz-Altendorf, St. Egidien, Zwickau). Quartz revealed even more unspecific characteristics, except for the samples from Chemnitz-Furth and St. Egidien, both showing a step at around 300 °C with mass loss of 0.1%–0.2%.

#### 3.1. Detected Compounds

##### 3.1.1. Hydrogen

Hydrogen does not occur separately but mainly results from splitting off from a compound after ionization. The remaining hydrogen either appears as H or H<sub>2</sub> on the  $m/q = 1$  and 2 (Figure 3), which also represent the mass-charge-ratios that identify hydrogen. Both H and H<sub>2</sub> mainly appear around 500–550 °C though H<sub>2</sub> often appears around 900–950 °C as well.

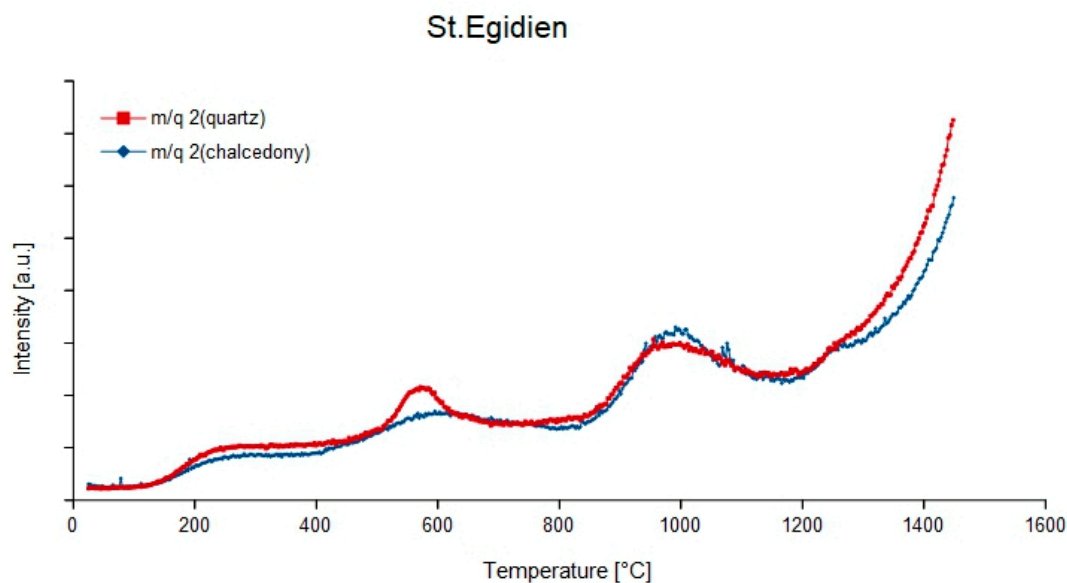


**Figure 3.** Temperature dependent degassing curves of the mass-charge ratio 2 ( $^1\text{H}_2$ ) of quartz and chalcedony in agate from St. Egidien, Germany.

### 3.1.2. Chlorine

Chlorine occurs on the mass-charge-ratios 35 and 37. The main part (75.8%) belongs to  $^{35}\text{Cl}$ , which is consistent with the mass-charge-ratio 35. The rest is associated with  $^{37}\text{Cl}$  (24.2%) [30]. The  $\text{Cl}_2$  molecule appears on the mass-charge-ratios 70, 72 (for  $^{36}\text{Cl}$  which is not stable or  $^{35}\text{Cl}^{37}\text{Cl}$ ) and 74, respectively. Together with H, chlorine forms  $\text{HCl}$ , which is detectable on the mass-charge-ratios 36 (Figure 4), 37 and 38 (Figure 5). In chalcedony, all mass-charge-ratios for chlorine could be identified except for the mass-charge-ratio = 35, which only occurred in the Rio Grande do Sul sample. However, in quartz all mass-charge-ratios could be identified, although  $m/q = 35$  only occurs in the samples Chemnitz-Furth, St. Egidien and Rio Grande do Sul. The measurements showed that all compounds degas between 300–500 °C and around 1000 °C. The identification is difficult due to the interference with other compounds. The mass-charge-ratios 35 and 36 can be interfered by  $\text{H}_2\text{S}$ , 37 by  $^{12}\text{C}_3^1\text{H}$  and 38 by  $^{19}\text{F}_2$  and  $^{12}\text{C}_3^1\text{H}_2$ . All chlorine molecules show interference with hydrocarbon compounds and with  $\text{SO}_2$ .

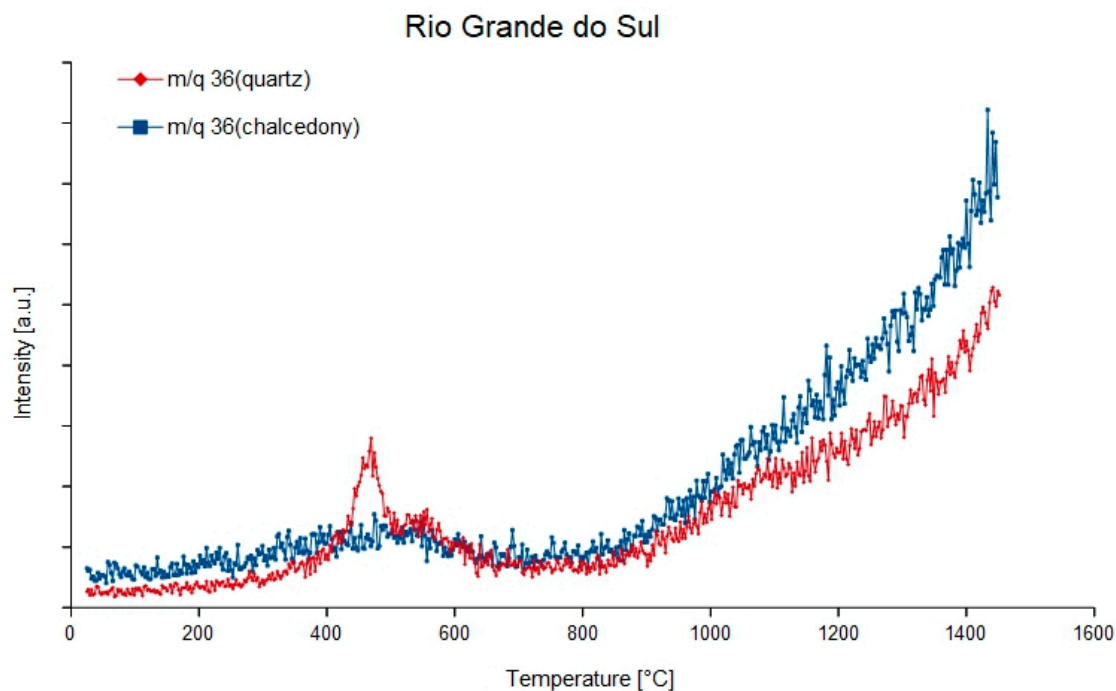


**Figure 4.** Degassing curves of the mass-charge ratio 36 ( $^1\text{H}^{35}\text{Cl}$ ) of quartz and chalcedony in agate from Rio Grande do Sul, Brazil.

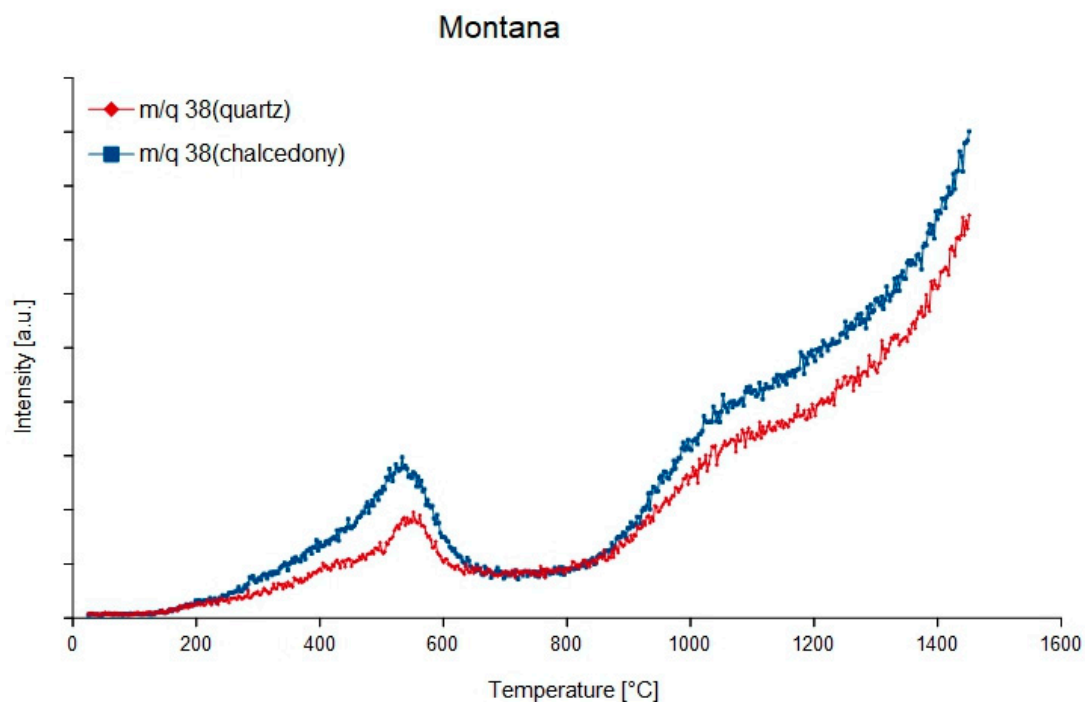


**Figure 5.** Degassing curves of the mass-charge ratio 38 ( $^1\text{H}^{37}\text{Cl}$ ) of quartz and chalcedony in sedimentary agate from Montana, USA.

### 3.1.3. Nitrogen

Nitrogen occurs as  $^{14}\text{N}$  and  $^{15}\text{N}$ , though  $^{15}\text{N}$  only makes 0.4% of the natural nitrogen. The nitrogen molecule  $^{14}\text{N}_2$  can be identified on the mass-charge-ratio 28 which is more abundant besides 29.  $\text{NO}$ ,  $\text{N}_2\text{O}$  and  $\text{NO}_2$  can be formed with oxygen and can be identified by the mass-charge-ratios 30

( $^{14}\text{N}^{16}\text{O}$ ), 44 and 45 ( $\text{N}_2\text{O}$ ) and 46 ( $^{14}\text{N}^{16}\text{O}_2$ ).  $\text{N}_2\text{O}$  and associated fragments show dominant peaks at  $m/q = 44, 30, 16$  and  $14$  (Figure 6), whereas in  $\text{NO}_2$  appears at  $m/q = 30, 46, 16$  and  $14$ . In combination with hydrogen,  $^{14}\text{N}^1\text{H}_3$  is formed with  $m/q = 14\text{--}17$ , with the peak at  $m/q = 17$  as the dominant. The main temperatures of degassing peak around  $500\text{ }^\circ\text{C}$  and around  $900\text{ }^\circ\text{C}$ . The nitrogen compounds show a variety of peak developments. In some samples (Zwickau, St. Egidien—see Figure 7) no peak was formed but a continuous curve occurs, especially at the mass-charge ratios 28, 30 and 44. Sometimes, strongly increasing curves appear (e.g.,  $m/q = 44, 45$  and  $46$  in Figure 8) and only a few samples exhibit well developed peaks (e.g., quartz in sample Chemnitz Furth and Rio Grande do Sul, respectively). A problem when identifying these compounds is the fact, that all of them (except  $m/q = 31$  for  $^{15}\text{N}^{16}\text{O}$ ) interfere with compounds of carbon.

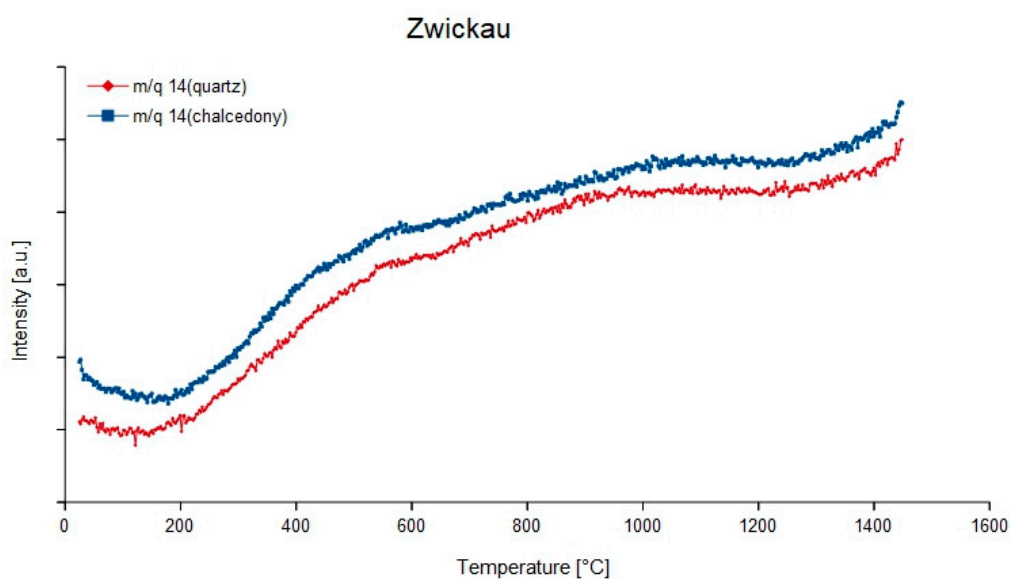


**Figure 6.** Continuous degassing curves of mass-charge ratio 14 (N) of the quartz and chalcedony parts in the agate from Zwickau, Germany.

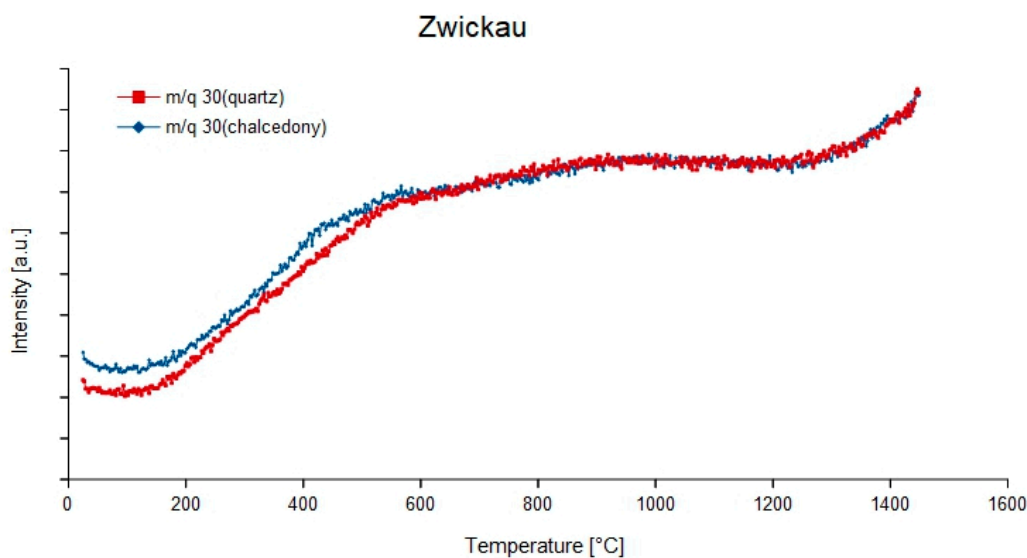


**Figure 7.** Continuous degassing curves of mass-charge ratio 30 ( $^{14}\text{N}^{16}\text{O}$ ) of the quartz and chalcedony parts in the agate from Zwickau, Germany.

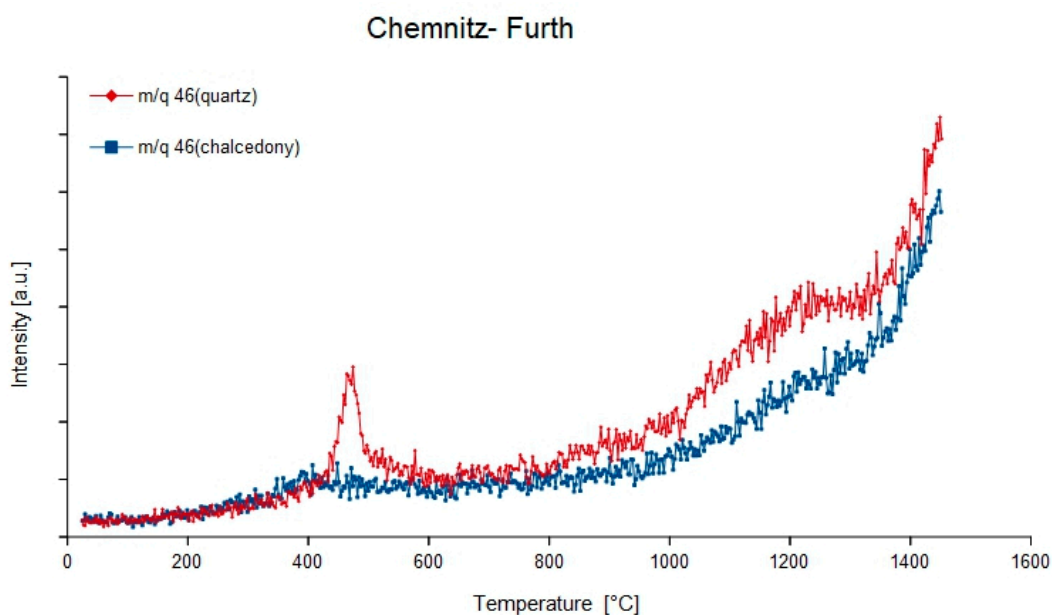


**Figure 8.** Degassing curves of the mass-charge ratio 46 ( $^{14}\text{N}^{16}\text{O}_2$ ) of quartz and chalcedony in the agate sample from Chemnitz- Furth, Germany.

### 3.1.4. Fluorine

Fluorine compounds are associated with the mass-charge-ratios 19 to 21 ( $\text{F} = 19$ ,  $\text{HF} = 20$  and 21). The fluorine molecule  $^{19}\text{F}_2$  appears at the mass-charge ratio 38. The degassing temperature was found mainly around 500 °C but also rises up to 1000 °C. Results of [20] with degassing temperatures around 900 °C confirm the recent measurements. Due to their overlap with water ( $m/z = 18\text{--}20$ ) the curves for  $^{19}\text{F}$  and  $^1\text{H}^{19}\text{F}$  do not show one clear peak but either several peaks (e.g., Rio Grande do Sul, St. Egidien in Figure 9) or a continuous curve of degassing. The interference of water with  $^{19}\text{F}$  and  $^1\text{H}^{19}\text{F}$  might be low but cannot be ignored.  $^{19}\text{F}_2$  interferes with  $^1\text{H}^{37}\text{Cl}$  and  $^{12}\text{C}_3^1\text{H}_2$ .

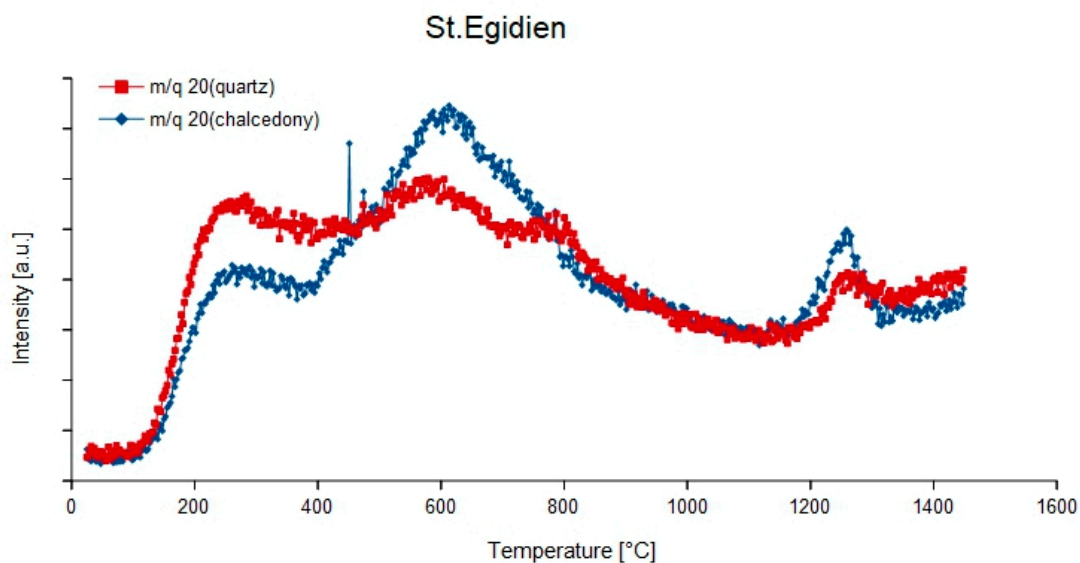


**Figure 9.** Degassing curves of the mass-charge ratio 20 ( $^1\text{H}^{19}\text{F}$ ) of quartz and chalcedony in the agate sample from St. Egidien, Germany.

### 3.1.5. Carbon

Carbon has the mass-charge ratios 12 and 13. The intensity on  $m/q = 12$  should be significantly higher than that on  $m/q = 13$ . Several hydrocarbon compounds are formed in combination with H as well as CO and CO<sub>2</sub> with oxygen. They can be identified via the mass-charge ratios 28 (Figure 10) and 44 which should show the highest intensity in comparison with other mass-charge ratios such as  $m/q = 12$  (<sup>12</sup>C), 16 (<sup>16</sup>O), 29 (<sup>13</sup>C<sup>16</sup>O), 45 (<sup>13</sup>C<sup>16</sup>O<sub>2</sub>) or 46 (<sup>12</sup>C<sup>17</sup>O<sub>2</sub>). Furthermore, carbonic acid (<sup>1</sup>H<sub>2</sub><sup>12</sup>C<sup>16</sup>O<sub>3</sub>) is another compound formed with hydrogen and oxygen. It is detectable on the mass-charge-ratio 62 and the dissociation products on 61(<sup>1</sup>H<sup>12</sup>C<sup>16</sup>O<sub>3</sub><sup>-</sup>) and 60 (<sup>12</sup>C<sup>16</sup>O<sub>3</sub><sup>2-</sup>—Figure 11).

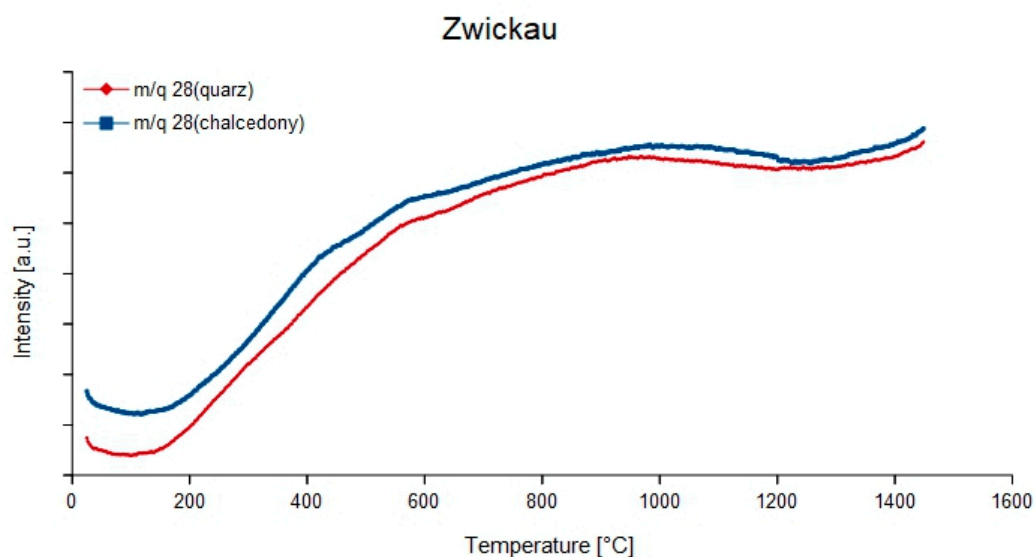


**Figure 10.** Continuous degassing curves of mass-charge ratio 28 (<sup>12</sup>C<sup>16</sup>O) of the quartz and chalcedony parts in the agate from Zwickau, Germany.

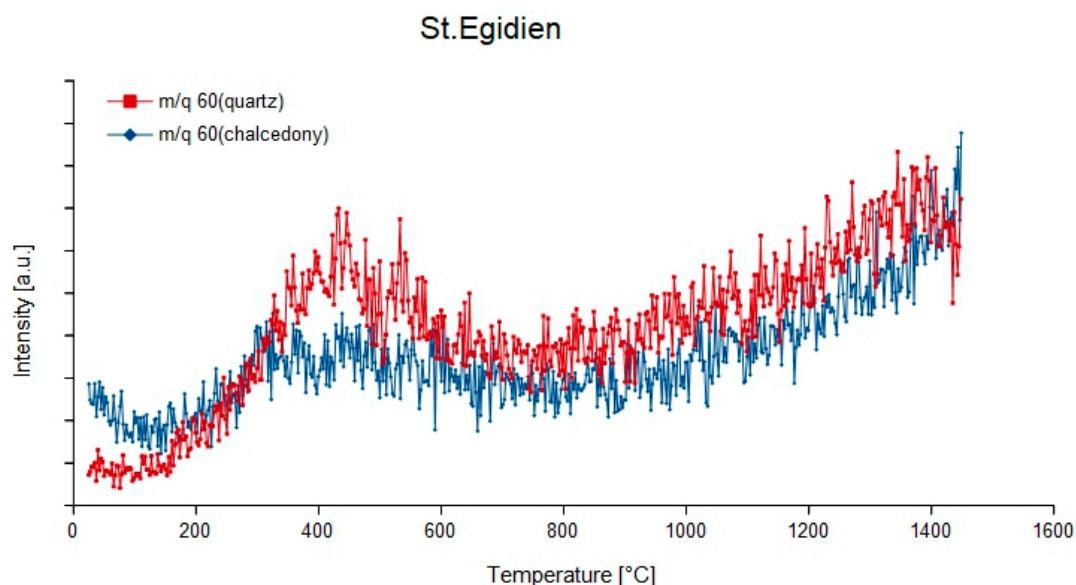


**Figure 11.** Degassing curves of  $m/q = 60$  (<sup>12</sup>C<sup>16</sup>O<sub>3</sub><sup>2-</sup>) of quartz and chalcedony in agate from St. Egidien, Germany.

Hydrocarbon compounds can also be present in hydrothermal and volcanic fluids. Studies of [31] detected hydrocarbon in agates of acidic volcanic rocks from Nowy Kosciol (Poland). The most

important hydrocarbon compounds are methane ( $^{12}\text{C}^1\text{H}_4$ ,  $m/q = 12$ ), ethane ( $^{12}\text{C}_2^1\text{H}_6$ ,  $m/q = 30$ ), propane ( $^{12}\text{C}_3^1\text{H}_8$ ,  $m/q = 44$ ), butane ( $^{12}\text{C}_4^1\text{H}_{10}$ ,  $m/q = 58$ ), heptane ( $^{12}\text{C}_5^1\text{H}_{12}$ ,  $m/q = 72$ ), hexane ( $^{12}\text{C}_6^1\text{H}_{14}$ ,  $m/q = 86$ ) and heptane ( $^{12}\text{C}_7^1\text{H}_{16}$ ,  $m/q = 100$ ). During ionization hydrogen splits up from the compounds and several dissociation products can form.

Looking at the degassing curves, either distinct peaks or exponential-like increasing curves can occur. The exponential increase is characteristic for the mass-charge ratios 12 ( $^{12}\text{C}$ , Figure 12), 28 ( $^{12}\text{C}^{16}\text{O}$ ) and 44 ( $^{12}\text{C}^{16}\text{O}_2$ ) in most samples except the agate from Chemnitz Furth ( $m/q = 12$  and 44). All other compounds degas at temperatures around 500 °C with slight differences between quartz and chalcedony. An exception is  $m/q = 60$  ( $^{12}\text{C}^{16}\text{O}_3^{2-}$ ), which was only detected in chalcedony of the samples from Montana, Rio Grande do Sul, Zwickau, St. Egidien and Schlottwitz at 300–400 °C and in the quartz fraction of all samples around 400 °C. At higher temperatures (1000 °C) only hydrocarbon compounds degas.

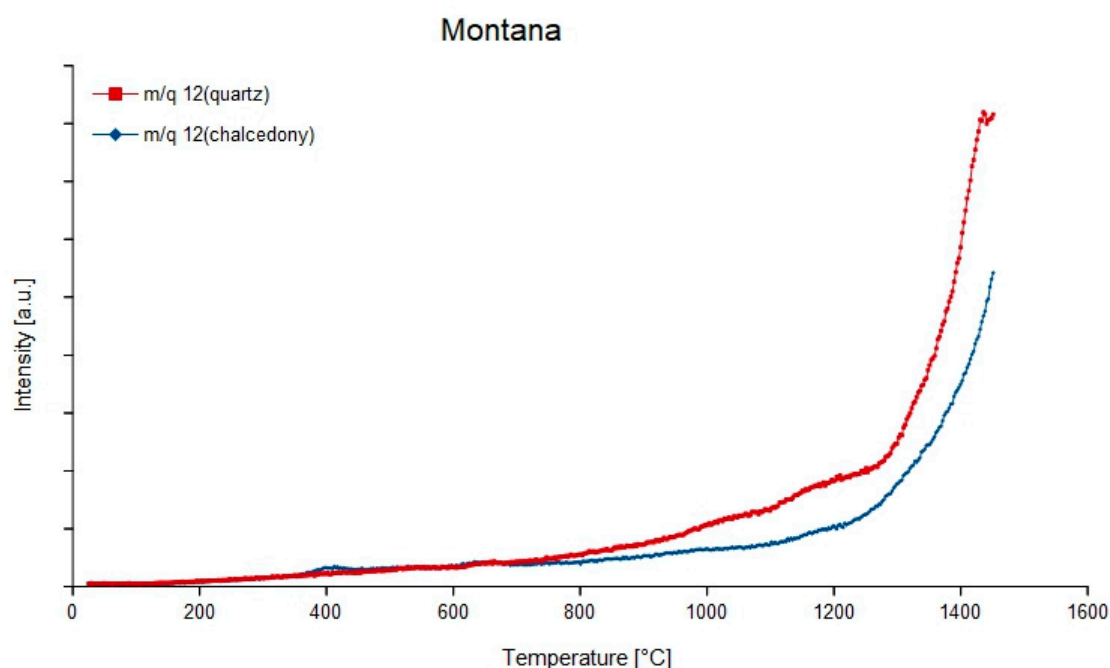


**Figure 12.** Degassing curves  $m/q = 12$  (C) of quartz and chalcedony from the Montana agate showing exponential shape.

Due to their complexity, carbon compounds interfere with many other compounds. For instance,  $^{12}\text{C}^{16}\text{O}$  and  $^{12}\text{C}^{16}\text{O}_2$  interfere with the nitrogen compounds  $^{14}\text{N}_2$ ,  $^{14}\text{N}_2^{16}\text{O}$  and  $^{14}\text{N}^{16}\text{O}_2$ , heptane with chlorine ( $m/q = 70, 72$ ), or sulphur compounds at high mass-charge ratios with other hydrocarbon compounds. Furthermore, different carbon compounds can interfere among each other such as  $^{12}\text{C}^{16}\text{O}$  and  $^{12}\text{C}_2^1\text{H}_4$  ( $m/q = 28$ —Figure 9) or  $^{12}\text{C}^{16}\text{O}_2$  and  $^{12}\text{C}_3^1\text{H}_8$  ( $m/q = 44$ ).

### 3.1.6. Sulphur

Natural sulphur consists of 95%  $^{32}\text{S}$ , 4.2%  $^{33}\text{S}$  and 0.75%  $^{34}\text{S}$  [30]. It can form compounds with hydrogen and oxygen, such as  $\text{SO}_2$ ,  $\text{H}_2\text{S}$ ,  $\text{H}_2\text{SO}_4$  and their decomposition products.  $\text{SO}_2$  can be identified with the mass-charge ratios 64 ( $^{32}\text{S}^{16}\text{O}_2$ , Figure 13), 48 ( $^{32}\text{S}^{16}\text{O}$ ) and 32 ( $^{32}\text{S}$ ), which are the most important besides 65, 50, 49, 34 and 33.  $\text{H}_2\text{S}$  should show the highest intensities on the mass-charge ratios 34 ( $^1\text{H}_2^{32}\text{S}$ , Figure 14), 35 ( $^1\text{H}_2^{33}\text{S}$ ) and 32 ( $^{32}\text{S}$ ), whereas  $m/q = 35$  and 36 have lower intensities.  $\text{H}_2\text{SO}_4$  is detectable on the mass-charge ratios 80 (Figure 15), 81, 82, 98, 64 and 65, which are important for identification.

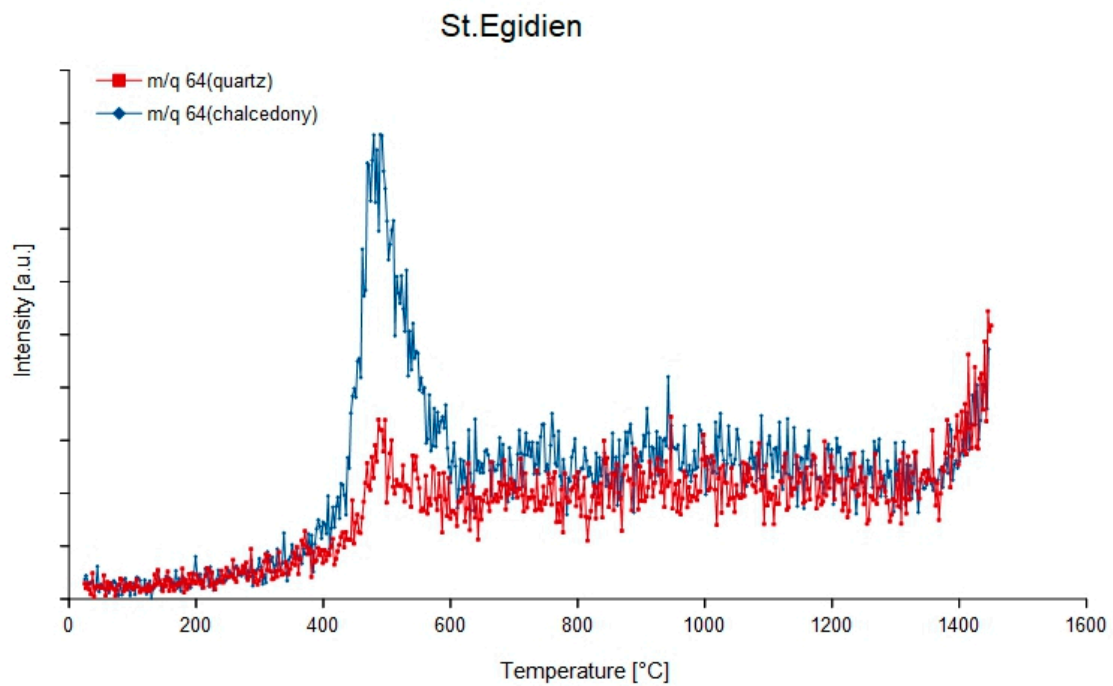


**Figure 13.** Degassing curves of quartz and chalcedony from the agate sample St. Egidien, Germany at mass-charge ratio 64 ( $^{32}\text{S}^{16}\text{O}_2$ ).

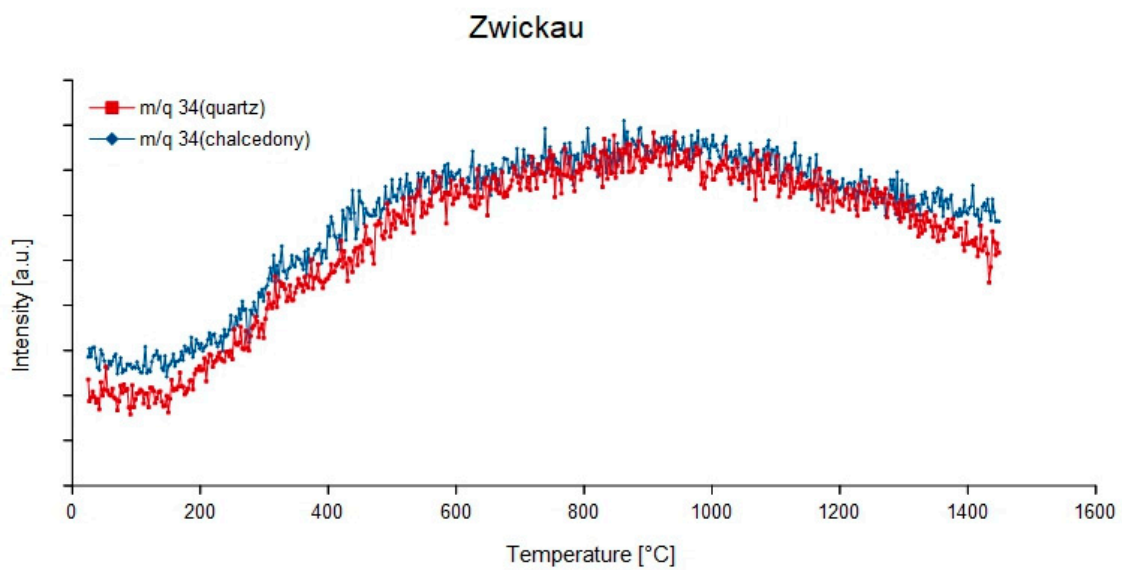


**Figure 14.** Continuous degassing curves of quartz and chalcedony in the agate from Zwickau, Germany at mass-charge ratio 34 ( $^1\text{H}_2^{32}\text{S}$ ).

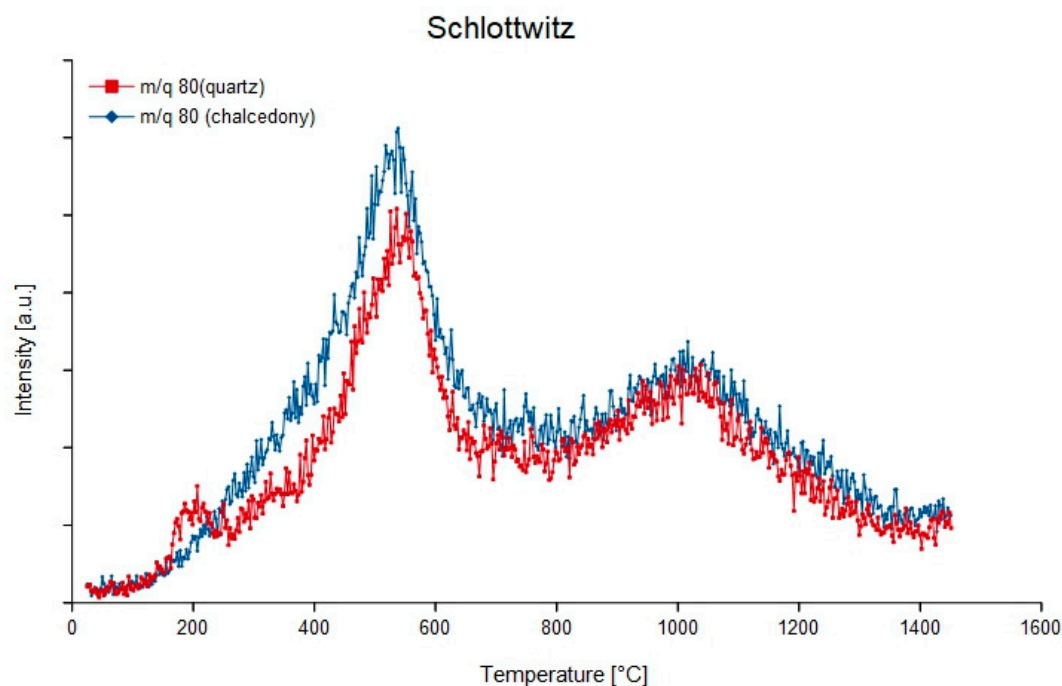


**Figure 15.** Degassing curves of quartz and chalcedony from the hydrothermal vein agate of Schlottwitz, Germany at mass-charge ratio 80 ( $^1\text{H}_2^{32}\text{S}^{16}\text{O}_4$ ).

Most sulphur compounds degas at low temperatures between 300 and 350 °C such as  $^{32}\text{S}^{16}\text{O}$  ( $m/q = 48$ ),  $^1\text{H}_2^{32}\text{S}$  ( $m/q = 34$ ) and  $\text{S}$  ( $m/q = 33$ ). The mass-charge ratio 64 often shows no distinct degassing peak but a strongly increasing curve, except for the agate from St. Egidien which shows a strong peak around 500 °C. For the  $m/q = 32$ , which only occurs in the chalcedony samples Rio Grande do Sul, St. Egidien and Zwickau, a curve with concave shape to the underground appears. In the quartz samples, this mass-charge ratio is not detectable in the agate from Chemnitz Furth.

Sulphur compounds show interferences with chlorine compounds, e.g., on the mass-charge ratios 35 ( $^1\text{H}_2^{33}\text{S}$  and  $^{35}\text{Cl}$ ) and 36 ( $^1\text{H}_2^{34}\text{S}$  and  $^1\text{H}^{35}\text{Cl}$ ) and with hydrocarbon compounds (except  $^{33}\text{S}$   $m/q = 33$  and  $^{32}\text{S}^{16}\text{O}$   $m/q = 48$ ).

### 3.2. Volatiles Compounds in Agates of Different Origins

#### 3.2.1. Agates from Mafic Volcanic Rocks

The agates from Rio Grande do Sul (Brazil) and Heads of Ayr (Scotland) originate from mafic volcanic rocks (basalts). The quartz part of the Rio Grande agate degasses between 250 and 550 °C with no degasification at a higher temperature range, whereas chalcedony of these samples shows degassing between 850 and 1300 °C. In contrast, both quartz and chalcedony from Heads of Ayr degas at low and high temperatures. The lower temperature range is between 150 and 600 °C with a maximum of degassing at 500 °C. At higher temperatures between 950 and 1200 °C only few volatiles could be detected (mainly hydrocarbon compounds). Both samples contain various sulphur-, chlorine- and hydrocarbon compounds as well as HF only in chalcedony.

#### 3.2.2. Agates from Acidic and Intermediate Volcanic Rocks

Agates originating from acidic to intermediate volcanic rocks are represented by the samples from Zwickau, Chemnitz-Furth and St. Egidien, Germany. Two main ranges of degasification were detected at 400–500 °C and 900–1000 °C with some additional compounds degassing between. Chalcedony tends

to degas at slightly higher temperatures (up to 1250 °C, Zwickau), whereas the escape temperatures of volatiles in macrocrystalline quartz are mostly below 1000 °C.

All samples contain compounds of nitrogen, chlorine, sulphur and carbon. The fluorine compounds  $^{19}\text{F}$  and  $^{19}\text{F}_2$  were detected in all samples, whereas  $^1\text{H}^{19}\text{F}$  was only found in the chalcedony separates. Carbonates were detected as well, preferentially in quartz. For instance,  $\text{H}_2\text{CO}_3$  and associated fragmentary compounds were measured during degassing of macrocrystalline quartz in the agate from Chemnitz Furth.

### 3.2.3. Vein Agates

Vein agates are represented by the samples from Chemnitz Altendorf and Schlottwitz. Both investigated agates contain sulphur and chlorine compounds as well as  $^1\text{H}_2^{12}\text{C}^{16}\text{O}_3$ . In addition,  $^{19}\text{F}$  and  $^{19}\text{F}_2$  were detected in the Chemnitz-Altendorf sample and  $^{12}\text{C}^{16}\text{O}_3^{2-}$ ,  $^1\text{H}^{12}\text{C}^{16}\text{O}_3$  as well as nitrogen compounds in the agate from Schlottwitz.

The agate from Chemnitz Altendorf showed a narrow temperature range of degasification. Both chalcedony and quartz mainly degas at 500 °C, quartz shows an additional escape of volatiles at a temperature of ca. 1000 °C (up to 1200 °C). The thermal behaviour of the agate from Schlottwitz is quite different. Volatiles in macrocrystalline quartz show narrow degassing temperature ranges around 250, 550 and 1000 °C, whereas chalcedony starts to degas in a wider range between 300 and 500 °C up to 950–1250 °C with some mass-charge-ratios showing additional escaping fluids in the temperature range between.

### 3.2.4. Sedimentary Agates

The agate from Montana, USA is also known as Dryhead agate which is formed in sedimentary rocks [26]. In this agate type compounds of nitrogen, chlorine, fluorine, sulphur and carbonate were detected. Chalcedony seems to contain more nitrogen compounds ( $^{14}\text{N}^1\text{H}_3$  and  $^{14}\text{N}^1\text{H}_2$ ), whereas fluorine ( $^{19}\text{F}$ ) is more abundant in macrocrystalline quartz.

Between 200–600 °C and 900–1050 °C, maxima of degassing were detected in both chalcedony and macrocrystalline quartz, although the escape of fluids from quartz occurred in a narrower range with a maximum around 500 °C. Chalcedony on the other hand shows varying maxima of degassing. Both show additional slight degasification between or above these temperature ranges on some mass-charge-ratios.

## 4. Discussion

The results of the experiments illustrate that there is a number of fluids present in chalcedony and macrocrystalline quartz of agates of different genetic types and from different occurrences worldwide. The main compounds together with the corresponding degassing temperatures are summarized in Table 2. It has to be considered that the chemical compounds listed are not identical with the primary fluids included in the agate samples. During degassing and ionization of the fluids at elevated temperature, processes of dissociation can change the original chemical composition of the compounds. Therefore, the detected compounds provide only indications regarding the chemical composition of the included fluids.

**Table 2.** Detected compounds and corresponding temperatures of degassing in the investigated agate samples.

Sample	Material	Compounds	Temperature (°C)
Rio Grande do Sul	Quartz	$^{14}\text{N}^{16}\text{O}$ , SO, S, $^{12}\text{C}^{16}\text{O}$ , $^{12}\text{C}^1\text{H}$ , $^1\text{H}^{19}\text{F}$	400–450
	Chalcedony	$^{14}\text{N}^{16}\text{O}$ , SO, S, $^{12}\text{C}^{16}\text{O}_3^{2-}$ , $^{12}\text{C}^1\text{H}$	150–500; 900–1050
Heads of Ayre	Quartz	$^{14}\text{N}^{16}\text{O}$ , SO, $^{12}\text{C}^{16}\text{O}_3^{2-}$ , $^{12}\text{C}^1\text{H}$	400; 600
	Chalcedony*		400; 500
Zwickau	Quartz	$^{14}\text{N}^{16}\text{O}$ , SO, $^{12}\text{C}^{16}\text{O}_3^{2-}$	400–500; 900–1000
	Chalcedony	$^{14}\text{N}^{16}\text{O}$ , $^{12}\text{C}^{16}\text{O}_3^{2-}$	400–500; 900–1000
Chemnitz Furth	Quartz	$^{14}\text{N}^{16}\text{O}$ , $^{14}\text{N}^{16}\text{O}_2$ , SO, S, $^{12}\text{C}^{16}\text{O}_3^{2-}$ , $^{12}\text{C}^1\text{H}$ , $^{12}\text{C}$ , $^1\text{H}^{19}\text{F}$	500; 1000
	Chalcedony	SO, $^{12}\text{C}^1\text{H}$	500; 1000
St. Egidien	Quartz	$^{14}\text{N}^{16}\text{O}$ , SO, $^{12}\text{C}^{16}\text{O}_3^{2-}$ , $^{12}\text{C}^1\text{H}$ , $^1\text{H}^{19}\text{F}$	400–500; 950–1000
	Chalcedony	$^{14}\text{N}^{16}\text{O}$ , SO, $^{12}\text{C}^{16}\text{O}_3^{2-}$ , $^{12}\text{C}^1\text{H}$	400–500; 900–1000
Montana	Quartz	$^{14}\text{N}^{16}\text{O}$ , SO, S, $^{12}\text{C}^{16}\text{O}_3^{2-}$ , $^{12}\text{C}^1\text{H}$	200–400; 500; 1000
	Chalcedony	$^{14}\text{N}^{16}\text{O}$ , SO, $^{12}\text{C}^{16}\text{O}_3^{2-}$ , $^{12}\text{C}^1\text{H}$	300–500; 1000
Chemnitz Altendorf	Quartz	$^{14}\text{N}^{16}\text{O}$ , SO, S, $^{12}\text{C}^{16}\text{O}_3^{2-}$ , $^{12}\text{C}^1\text{H}$ , $^1\text{H}^{19}\text{F}$	500; 1000
	Chalcedony	$^{14}\text{N}^{16}\text{O}$ , SO, S, $^{12}\text{C}^{16}\text{O}$ , $^{12}\text{C}^1\text{H}$ , $^1\text{H}^{19}\text{F}$	500
Schlottwitz	Quartz	$^{14}\text{N}^{16}\text{O}$ , SO, S, $^{12}\text{C}^{16}\text{O}_3^{2-}$ , $^{12}\text{C}^1\text{H}$	500; 1000
	Chalcedony	$^{14}\text{N}^{16}\text{O}$ , SO, $^{12}\text{C}^{16}\text{O}_3^{2-}$ , $^{12}\text{C}^1\text{H}$	300–350; 450–500; 950–1000

\* The chalcedony separated from the Heads of Ayre sample did not provide properly identifiable compounds due to interferences.

The degassing curves (Figures 3–15) illustrate that the escape of fluids can occur in two different ways: abruptly or as diffusion process. Sharp peaks (spikes) are interpreted to be explosion-like decrepitation effects due to the rupture of inclusions, caused by the increasing pressure in the inclusions and resulting in abrupt degassing [32]. On the other hand, a steeply rising curve is assumed to be correlated with the opening of cracks (around 800 °C). Whereas the spikes were detected at varying temperatures, in our samples the crack-correlated increase of the signals occurred around 500 and 900 °C respectively.

Diffusion, on the other hand, results in broad maxima because of a rather slow and continuous process of volatile release. It occurs when structurally bound molecules diffuse out of the quartz structure at a certain temperature. The simultaneous occurrence of crack opening and diffusion processes causes defined peaks with a broad foot, which are found for most mass-charge ratios [33,34].

The chemical composition of fluids found in nearly all samples is characterized by carbonates, nitrogen-, sulphur- and fluorine compounds as indicated in Table 2. Furthermore, chlorine was found though it shows interference with other compounds. Its presence, especially the mass-charge ratio 35, was verified by Götze et al. [19], who found chlorine as a salt in the inclusions of the samples Chemnitz-Furth and St. Egidien.

Although there was no marked difference in abundance of measured fluid compounds between quartz and chalcedony the mass charge ratios measured in quartz occurred at more temperature ranges. In addition, carbonates seem to appear more commonly in macrocrystalline quartz, whereas fluorine compounds were more frequently detected in chalcedony.

Except for the sample Heads of Ayre, the investigated samples, show two ranges of degasification for both chalcedony and macrocrystalline quartz. Most compounds escape in the lower temperature range around 500 °C. At higher temperatures between 950–1050 °C mainly hydrocarbon compounds, carbonates and sulphur compounds were detected. Chalcedony showed additional degassing between 150 to 350 °C and 1100 to 1250 °C, which is interpreted as degassing from liquids from grain boundaries and enclosed inclusions.

Differences were detected for agate samples from different genetic environments, in particular when comparing the temperatures of degassing. In general, agates from mafic volcanic rocks tend to have a broad temperature range of degassing, whereas the agates of felsic origin show a narrower one. The first release of volatiles happens around 500 °C, the second degassing around 1000 °C is more pronounced in the agates from felsic host rocks. Agates from a sedimentary host rock show two temperature ranges of degassing with the lower one between 200 and 500 °C. These different

degassing temperatures show that differences in the agate micro-structure may influence the thermal release of fluids. A looser structure results in degassing at lower temperatures.

In general, the results from a recent study [35] are confirmed by this investigation. Moxon [35] differentiated between different types of water with distinct degassing temperatures (e.g., molecular water <190 °C and silanol water >1000 °C). Although the focus in the present study was more on the different compounds that evolve during heating, distinct temperature ranges were also found for both the mass loss and the detected components (see Table 2). Differences in the temperatures that were described in detail in [35] and the presented data may be found in the different design and objective of the experiments.

An interesting result is the possible role of chlorine and fluorine compounds in the transport and accumulation of silica and other elements during agate formation [20]. Both compounds could be detected, although the presence of chlorine is uncertain due to the strong interference with other compounds. Nevertheless, the results indicate the possible transport of silica in other forms than as diffusing silicic acid in aqueous pore solutions. Such a scenario is emphasized by Schrön [21], who proposed the volatile transport of silica as  $\text{SiF}_4$ .

The results in Table 2 emphasize that fluorine compounds were in particular detected in agates from volcanic environments. This can be explained by the preferred occurrence of F-bearing volatiles in volcanic processes, which can act as transport media for certain chemical compounds. Götze et al. [20] detected high concentrations of Ge, U and B in agates of acidic volcanic rocks and concluded that other fluids than aqueous ones can play a role in the alteration of volcanic rocks and the mobilization and transport of  $\text{SiO}_2$  and other chemical compounds. Chemical transport reactions by stable fluorine compounds such as  $\text{SiF}_4$ ,  $\text{BF}_3$ ,  $\text{GeF}_4$  and  $\text{UO}_2\text{F}_2$  could be responsible for the accumulation of these elements and additional phases such as calcite or fluorite besides  $\text{SiO}_2$  modifications in volcanic agates. Accordingly, element transport for agate formation in volcanic environments is not exclusively related to aqueous solutions.

The results of the present study also provided some more information regarding the participation of different fluids during the formation of the agates. The occurrence of hydrocarbon compounds in agates of volcanic origin was proven, which was first suggested by Dumańska-Słowik et al. [31] and Götze et al. [20]. In the case of the agates from Nowy Kościół (Poland), Dumańska-Słowik et al. [31] detected solid bitumen, which they related to algal or a mixed algal-humic origin based on the stable carbon isotope composition.

In the agates investigated in this study, certain hydrocarbon compounds as well as carbonic acid could be detected. The incorporation of hydro-carbon compounds as inclusions into the  $\text{SiO}_2$  microstructure points to co-precipitation of both materials, probably from the same source. Hydrothermal methane and/or higher-molecular hydrocarbon compounds in the volatiles participating in the silica accumulation could have served as precursors for the detected organic fluids in the agate.

## 5. Conclusions

Separated chalcedony and macrocrystalline quartz from eight agates of different origin and localities were analysed by thermoanalysis directly coupled with a mass spectrometer. The temperature ranges at which degassing occurs were mainly found around 500 and 1000 °C. The analysed volatiles consisted of compounds of C, N, S, F and Cl with H and/or O. They could be identified according to their specific mass-charge ratio and the corresponding temperature of degassing. Due to interferences of different compounds with similar mass-charge ratios not all compounds could be definitely identified. Nevertheless, the results gave indications regarding the sources and transport of silica for the agate formation. Besides the transport and accumulation of silica in aqueous solutions, the possible role of fluorine compounds,  $\text{CO}_2$  and other fluids in the alteration of rocks and the mobilization and transport of  $\text{SiO}_2$  have to be taken into account.

The method of thermogravimetry-mass-spectrometry used is suitable for the investigation of fluid phases in minerals because of the limited requirements for preparation and the possibility for direct measurements of escaping gases. However, limitations in the proper verification of chemical compounds are given by interfering mass-charge-ratios due to the limited resolution of the mass-spectrometer. Moreover, the measured chemical compounds are not always identical with the primary included fluids, since ionization and dissociation of the volatiles at elevated temperatures can change the original chemical composition of the compounds. Therefore, the detected compounds often represent fragments of the primary volatiles.

**Acknowledgments:** We are grateful to Terry Moxon (Doncaster, UK) for providing samples of Scottish agates. The reviews of T. Moxon, an anonymous reviewer, improved the quality of the paper significantly.

**Author Contributions:** Julia Richter-Feig and Robert Möckel prepared the samples and performed the measurements. Gerhard Heide provided the analytical equipment for the analysis and Jens Götze provided the samples. The results were analysed by Julia Richter-Feig and further evaluated by Robert Möckel, Jens Götze and Gerhard Heide. Julia Richter-Feig wrote the first draft of the paper and Jens Götze and Robert Möckel substantially revised it.

**Conflicts of Interest:** The authors declare no conflict of interest.

## References

1. Landmesser, M. Das Problem der Achatgenese. *Mitteilungen Pollichia* **1984**, *72*, 5–137. (In German)
2. Godovikov, A.A.; Ripinen, O.I.; Motorin, S.G. *Agaty*; Moskva, Nedra: Moscow, Russia, 1987; p. 368.
3. Blankenburg, H.-J. *Achat*; VEB Deutscher Verlag für Grundstoffindustrie: Leipzig, Germany, 1988; p. 203.
4. Moxon, T.; Rios, S. Moganite and water content as a function of age in agate: An XRD and thermogravimetric study. *Eur. J. Mineral.* **2004**, *4*, 693–706. [[CrossRef](#)]
5. Holzhey, G. Vorkommen und Genese der Achate und Paragenesminerale in Rhyolithkugeln aus Rotliegendevulkaniten des Thüringer Waldes. Ph.D. Thesis, TU Bergakademie Freiberg, Freiberg, Germany, 1993. (In German)
6. Pabian, R.K.; Zarins, A. *Banded Agates—Origins and Inclusions*; Educational Circular No. 12; University of Nebraska: Lincoln, NE, USA, 1994; p. 32.
7. Götze, J. Agate—Fascination between legend and science. In *Agates III*; Zenz, J., Ed.; Bode-Verlag: Salzhemmendorf, Germany, 2011; pp. 19–133.
8. Moxon, T.; Petrone, C.M.; Reed, S.J.B. Characterization and genesis of horizontal banding in Brazilian agate: An X-ray diffraction, thermogravimetric and electron microprobe study. *Mineral. Mag.* **2013**, *77*, 227–248. [[CrossRef](#)]
9. Moxon, T.; Reed, S.J.B. Agate and chalcedony from igneous and sedimentary hosts aged from 13 to 3480 Ma: A cathodoluminescence study. *Mineral. Mag.* **2006**, *70*, 485–498. [[CrossRef](#)]
10. Merino, E.; Wang, Y.; Deloule, E. Genesis of agates in flood basalts: twisting of chalcedony fibers and trace-element geochemistry. *Am. J. Sci.* **1995**, *295*, 1156–1176. [[CrossRef](#)]
11. Heaney, P.J. A proposed mechanism for the growth of chalcedony. *Contrib. Mineral. Petrol.* **1993**, *115*, 66–74. [[CrossRef](#)]
12. Graetsch, H. Structural characteristics of opaline and microcrystalline silica minerals. *Rev. Mineral. Geochem.* **1994**, *29*, 209–232.
13. Götze, J.; Nasdala, L.; Kleeberg, R.; Wenzel, M. Occurrence and distribution of “moganite” in agate/chalcedony: A combined micro-Raman, Rietveld and cathodoluminescence study. *Contrib. Mineral. Petrol.* **1998**, *133*, 96–105. [[CrossRef](#)]
14. Flörke, O.W.; Graetsch, H.; Martin, B.; Röller, K.; Wirth, R. Nomenclature of Micro- and Non-Crystalline Silica Minerals, Based on Structure and Microstructure. *Neues Jahrbuch Mineralogie Abhandlungen* **1991**, *163*, 19–42.
15. Breitkreuz, C. Spherulites and lithophysae—200 years of investigation on high-temperature crystallization domains in silica-rich volcanic rocks. *Bull. Volcanol.* **2013**, *75*, 705–720. [[CrossRef](#)]
16. Petránek, J. Sedimentäre Achate. *Der Aufschluss* **2009**, *60*, 291–302.
17. Holzhey, G. Herkunft und Akkumulation des SiO<sub>2</sub> in Rhyolithkugeln aus Rotliegendevulkaniten des Thüringer Waldes. *Geowissenschaftliche Mitteilungen von Thüringen* **1995**, *3*, 31–59. (In German)

18. Moxon, T. On the origin of agate with particular reference to fortification agate found in the Midland Valley, Scotland. *Chemie der Erde* **1991**, *51*, 251–260.
19. Götze, J.; Möckel, R.; Vennemann, T.; Müller, A. Origin and geochemistry of agates from Permian volcanic rocks of the Sub-Erzgebirge basin (Saxony, Germany). *Chem. Geol.* **2016**, *428*, 77–91.
20. Götze, J.; Schrön, W.; Möckel, R.; Heide, K. The role of fluids in the formation of agates. *Chemie der Erde* **2012**, *72*, 283–286. [[CrossRef](#)]
21. Schrön, W. Chemical fluid transport (CFT)—A window into Earth and its development. *Chemie der Erde* **2013**, *73*, 421–428. [[CrossRef](#)]
22. Gilg, H.A.; Morteani, G.; Kostitsyn, Y.; Preinfalk, C.; Gatter, I.; Strieder, A.J. Genesis of amethyst geodes in basaltic rocks of the Serra Geral formation (Ametista do Sul, Rio Grande do Sul, Brazil): A fluid inclusion, REE, oxygen, carbon and Sr isotope study on basalt, quartz and calcite. *Miner. Depos.* **2003**, *38*, 1009–1025. [[CrossRef](#)]
23. Phillips, E.R. *Petrology of the Igneous Rocks Exposed in the Ayr District (Sheet 14 W) of the Southern Midland Valley, Scotland*; British Geological Survey: Nottingham, UK, 1999.
24. Thirlwell, M.F. Geochronology of Late Caledonian magmatism in northern Britain. *J. Geol. Soc. Lond.* **1988**, *145*, 951–967. [[CrossRef](#)]
25. Haake, R.; Fischer, J.; Reissmann, R. Über die Achat - und Amethyst-Vorkommen von Schlottwitz im Osterzgebirge. *Mineralien-Welt* **1991**, *1*, 20–24.
26. Götze, J.; Möckel, R.; Kempe, U.; Kapitonov, I.; Vennemann, T. Characteristics and origin of agates in sedimentary rocks from the the Dryhead area, Montana, USA. *Mineral. Mag.* **2009**, *73*, 673–690. [[CrossRef](#)]
27. Heide, K. 1. Aufl. Leipzig. In *Dynamische Thermische Analysenmethoden*; Deutscher Verlag für Grundstoffindustrie: Leipzig, Germany, 1979.
28. Schöps, D.; Schmidt, C.M.; Heide, K. Quantitative EGA analysis of H<sub>2</sub>O in silicate glasses. *J. Therm. Anal. Calorim.* **2005**, *80*, 749–752. [[CrossRef](#)]
29. Otto, M. 3. Aufl. Weinheim. In *Analytische Chemie*; WILEY-VCH Verlag GmbH & Co. KGaA: Weinheim, Germany, 2006.
30. Faure, G.; Mensing, T.M. *Isotopes Principles and Application*; John Wiley & Sons: Hoboken, NJ, USA, 2005.
31. Dumańska-Słowik, M.; Natkaniec-Nowak, L.; Kotarba, M.J.; Sikorska, M.; Rzymelka, J.A.; Łoboda, A.; Gawęł, A. Mineralogical and geochemical characterization of the "bituminous" agates from Nowy Kościół (Lower Silesia, Poland). *N. Jb. Miner. Abh.* **2008**, *184*, 255–268. [[CrossRef](#)]
32. Barker, C.; Smith, M.P. Mass spectrometric determination of gases in individual fluid inclusions in natural minerals. *Anal. Chem.* **1986**, *58*, 1330–1333. [[CrossRef](#)]
33. Roedder, E. *Fluid Inclusions*; Reviews in Mineralogy Volume 12; Mineralogical Society of America: Chantilly, VA, USA, 1984; p. 646.
34. Lambrecht, G.; Diamond, L.W. Morphological ripening of fluid inclusions and coupled zone-refining in quartz crystals revealed by cathodoluminescence imaging: Implications for CL-petrography, fluid inclusion analysis and trace-element geothermometry. *Geochim. Cosmochim. Acta* **2014**, *141*, 381–406. [[CrossRef](#)]
35. Moxon, T. A re-examination of water in agate and its bearing on the agate genesis enigma. *Mineral. Mag.* **2017**, *81*, 1223–1244. [[CrossRef](#)]

